

Modeling alignment of electron trajectory in cooling section of EIC Low Energy Cooler

S. Seletskiy

October 2024

Electron-Ion Collider
Brookhaven National Laboratory

U.S. Department of Energy
USDOE Office of Science (SC), Nuclear Physics (NP)

Notice: This technical note has been authored by employees of Brookhaven Science Associates, LLC under Contract No. DE-SC0012704 with the U.S. Department of Energy. The publisher by accepting the technical note for publication acknowledges that the United States Government retains a non-exclusive, paid-up, irrevocable, world-wide license to publish or reproduce the published form of this technical note, or allow others to do so, for United States Government purposes.

DISCLAIMER

This report was prepared as an account of work sponsored by an agency of the United States Government. Neither the United States Government nor any agency thereof, nor any of their employees, nor any of their contractors, subcontractors, or their employees, makes any warranty, express or implied, or assumes any legal liability or responsibility for the accuracy, completeness, or any third party's use or the results of such use of any information, apparatus, product, or process disclosed, or represents that its use would not infringe privately owned rights. Reference herein to any specific commercial product, process, or service by trade name, trademark, manufacturer, or otherwise, does not necessarily constitute or imply its endorsement, recommendation, or favoring by the United States Government or any agency thereof or its contractors or subcontractors. The views and opinions of authors expressed herein do not necessarily state or reflect those of the United States Government or any agency thereof.

Modeling alignment of electron trajectory in cooling section of EIC Low Energy Cooler

S. Seletskiy*
Brookhaven National Laboratory

October 24, 2024

Contents

| | | |
|----------|---|-----------|
| 1 | Introduction | 2 |
| 2 | Factors contributing to trajectory misalignment | 3 |
| 2.1 | Trajectory correctors immersed into solenoid | 5 |
| 2.2 | Solenoid inclination | 6 |
| 2.3 | Shifted solenoid | 7 |
| 2.4 | Entering solenoid with misaligned trajectory | 8 |
| 2.5 | Misaligned BPMs | 9 |
| 2.6 | Fields in solenoid-BPM drift | 10 |
| 3 | Expected angles in the cooling section | 12 |
| 3.1 | Model of cooling section | 12 |
| 3.2 | Sanity checks | 12 |
| 3.3 | Average angles depending on combination of errors | 14 |
| 4 | Conclusion and discussion | 17 |

*seletskiy@bnl.gov

1 Introduction

The Electron Ion Collider (EIC) requires cooling of protons at the injection energy to obtain emittances needed to achieve the design luminosity. The low energy cooler (LEC) provides such a capability.

The LEC is an electron cooler [1] utilizing a non-magnetized, RF-based electron cooling. This approach to cooling was successfully used in Low Energy RHIC Electron Cooler (LEReC)[2, 3, 4, 5, 6].

A schematic layout of the LEC is shown in Fig. 1.

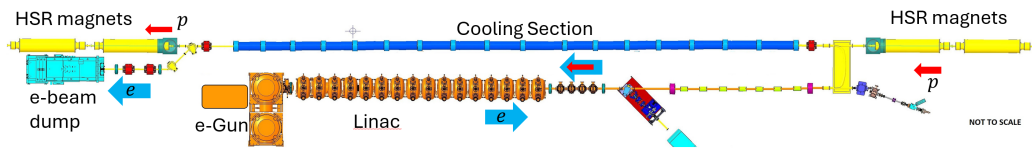


Figure 1: Layout of the EIC Low Energy Cooler.

In the LEC electrons are produced in a DC gun by illuminating a photocathode with a high frequency laser. The electrons are accelerated to $\gamma = 25.4$ and transported to a 170 m long cooling section (CS), where they co-travel with the proton bunches. After a single pass through the CS the electrons are dumped.

Main parameters of the cooler are listed in Table 1.

Table 1: Parameters of the EIC Low Energy Cooler

| | electrons | protons |
|---|----------------|---------|
| relativistic γ -factor | 25.4 | |
| cooling section length [m] | 170 | |
| normalized emittance (ε_n) [$\mu\text{m}\cdot\text{rad}$] | 1.5 | 2 |
| CS β -function [m] | 150 | 150 |
| bunch charge (Q_b) [nC] | 1.2×3 | 45 |
| rms longitudinal bunch length (σ_z) [cm] | 5 | 70 |

It is planned to overlap three electron bunches with one proton bunch. The protons will be stored in a flat-top bucket, which will allow to reduce their peak current by about a factor of two, as Fig. 2 demonstrates.

To obtain good cooling, the overall angles of electrons in the CS mustn't exceed $\Theta_{\max} = 30 \mu\text{rad}$. An angular spread of electron bunch in the cooling section due to its emittance is $\sigma_\theta \approx 20 \mu\text{rad}$. Then, assuming that the total angles can be found by adding the angular spread and the average

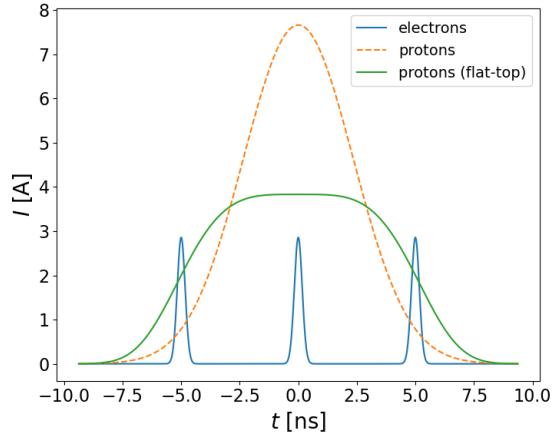


Figure 2: Longitudinal distribution of the proton and electron bunches in the cooling section.

trajectory angles in the CS in quadrature, we get the maximum tolerable average trajectory angle $\theta_{\max} = \sqrt{\Theta_{\max}^2 - \sigma_{\theta}^2} \approx 20 \mu\text{rad}$.

2 Factors contributing to trajectory misalignment

The electron trajectory through the cooling section will be defined by the CS proton trajectory. In the ideal case, one wants to have zero angle and displacement of electrons trajectory with respect to protons through the whole cooling section. In reality, there are multiple factors causing relative misalignment of electrons and protons.

The LEC cooling section consists of fourteen 12 meters long modules. Each module contains a short solenoid combined with horizontal and vertical dipole correctors [7], the long drift shielded by two layers of μ -metal [8] and a BPM. Main parameters of the CS module are listed in Table 2.

The electron beam trajectory can get misaligned with respect to the protons' trajectory because of inclination or transverse displacement of a solenoid (as schematically shown in Fig. 3). Misaligned solenoids create both a nonzero trajectory angle and a nonzero trajectory displacement at the solenoid's exit, which can not be ideally compensated by the dipole correctors.

Since an expected attenuation factor from the CS magnetic shielding is around 1000 [8], there is going to be a small dipole-like ambient transverse

Table 2: Parameters of a cooling section module

| | |
|---|---------|
| length of solenoid&correctors assembly (L) [cm] | 18.906 |
| solenoid current to field conversion factor (χ_s) [G/A] | 10.2365 |
| design solenoid field (B_s) [G] | 180 |
| corrector current to field conversion factor (χ_c) [G/A] | 0.5628 |
| maximum corrector current ($I_{c(\max)}$) [A] | 2 |
| distance from solenoid exit to BPM (Z) [m] | 12 |

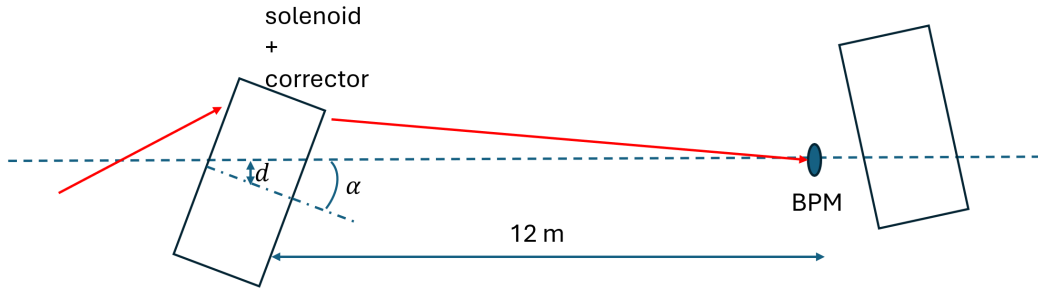


Figure 3: Solenoids misalignment (inclination α and transverse displacement d) in the cooling section

field in the solenoid to BPM drift, which also will contribute to average trajectory angles.

Additionally, in the cooling section the electrons are traveling in the focusing field created by the proton beam space charge. Therefore, as long as electron bunch centroid is transversely displaced with respect to the protons' trajectory, the electron trajectory will acquire an additional angle from the beam-beam kick (BBK) effect [6, 9].

Finally, the CS BPMs can have errors, which will also inevitably result in misalignment of electron and proton trajectories.

In this section we will consider individual contributions of various factors to e-p trajectory misalignment.

We will use a hard-edge approximation and model our solenoids by their transfer matrices:

$$M_s = \begin{pmatrix} \frac{1+C}{2} & \frac{S}{k} & \frac{S}{2} & \frac{1-C}{k} \\ -kS & 1+C & k(C-1) & \frac{S}{2} \\ -\frac{4}{S} & \frac{C-1}{k} & \frac{4}{1+C} & \frac{2}{S} \\ \frac{k(1-C)}{4} & -\frac{S}{2} & -\frac{kS}{4} & \frac{1+C}{2} \end{pmatrix} \quad (1)$$

where $C = \cos(kL)$, $S = \sin(kL)$, $k = \frac{B_s}{B\rho}$

Such an approximation is well justified for our solenoids as was shown both by comparison to tracking studies [10, 11] and by application of this model to trajectory correction in LEReC [6].

2.1 Trajectory correctors immersed into solenoid

Effect of a dipole corrector immersed into a solenoidal field on the trajectory is given by [10, 12]:

$$\vec{X}_c = \begin{pmatrix} \frac{B_{cy}(C-1)+B_{cx}(kL-S)}{B_s k} \\ \frac{B_{cx}(1-C)-B_{cy}(S+kL)}{2B_s} \\ \frac{B_{cx}(1-C)+B_{cy}(kL-S)}{B_s k} \\ \frac{B_{cy}(1-C)+B_{cx}(S+kL)}{2B_s} \end{pmatrix} \quad (2)$$

where B_{cx} and B_{cy} are transverse fields created by the corrector. Vector \vec{X}_c describes a trajectory $(x_c, x'_c, y_c, y'_c)^T$ at the exit of the solenoid-corrector combo.

A trajectory correction algorithm planned for the LEC (and successfully utilized in LEReC [6]) consists of zeroing the readings of a BPM located downstream of particular corrector.

Let us assume that the errors accumulated in the upstream beamline and the solenoid itself (due to its inclination and shift) result in the trajectory error at the solenoid exit represented by a vector $(x_{err}, x'_{err}, y_{err}, y'_{err})$. If this error is uncompensated, then the trajectory horizontal and vertical displacements in the downstream BPM are $x_{err} + x'_{err}Z$ and $y_{err} + y'_{err}Z$, where Z is the distance from the solenoid to the BPM. Then, the settings of the respective corrector must be such that:

$$\begin{aligned} x_c + x'_c Z &= \mathcal{X} \\ y_c + y'_c Z &= \mathcal{Y} \end{aligned} \quad (3)$$

where we define $\mathcal{X} \equiv -(x_{err} + x'_{err}Z)$ and $\mathcal{Y} \equiv -(y_{err} + y'_{err}Z)$.

Substituting Eq. (2) into Eq. (3) and solving the obtained system of equations for B_{cx} and B_{cy} , we get:

$$\begin{aligned} B_{cx} &= \frac{b\mathcal{X}+a\mathcal{Y}}{a^2+b^2} \\ B_{cy} &= \frac{b\mathcal{Y}-a\mathcal{X}}{a^2+b^2} \\ a &= \frac{1-C}{kB_s} + \frac{S+kL}{2B_s} Z, \quad b = \frac{kL-S}{kB_s} + \frac{1-C}{2B_s} Z \end{aligned} \quad (4)$$

Finally, substituting Eq. (4) back into Eq. (2), we obtain:

$$\begin{aligned}
x_c &= \frac{(b\mathcal{Y}-a\mathcal{X})(1-C)+(b\mathcal{X}+a\mathcal{Y})(kL-S)}{kB_s(a^2+b^2)} \\
x'_c &= \frac{(b\mathcal{X}+a\mathcal{Y})(1-C)+(a\mathcal{X}-b\mathcal{Y})(S+kL)}{2B_s(a^2+b^2)} \\
y_c &= \frac{(b\mathcal{X}+a\mathcal{Y})(1-C)+(b\mathcal{Y}-a\mathcal{X})(kL-S)}{kB_s(a^2+b^2)} \\
y'_c &= \frac{(b\mathcal{Y}-a\mathcal{X})(1-C)+(b\mathcal{X}+a\mathcal{Y})(S+kL)}{2B_s(a^2+b^2)}
\end{aligned} \tag{5}$$

2.2 Solenoid inclination

The effect of an inclined solenoid on the trajectory can be found as:

$$\vec{X}_\alpha = M_s \begin{pmatrix} -L\alpha_x/2 \\ \alpha_x \\ -L\alpha_y/2 \\ \alpha_y \end{pmatrix} - \begin{pmatrix} L\alpha_x/2 \\ \alpha_x \\ L\alpha_y/2 \\ \alpha_y \end{pmatrix} \tag{6}$$

where α_x, α_y are inclination angles with respect to the ideal e-beam trajectory.

As a result, we get for the trajectory at the exit of an inclined solenoid:

$$\vec{X}_\alpha = \begin{pmatrix} -\alpha_x \frac{(C-1)kL+4(kL-S)}{4k} - \alpha_y \frac{4(C-1)+kLS}{4k} \\ \alpha_x \frac{4(C-1)+kLS}{8} + \alpha_y \frac{(C-1)kL+4S}{8} \\ \alpha_x \frac{4(C-1)+kLS}{8} - \alpha_y \frac{(C-1)kL+4(kL-S)}{8} \\ \alpha_x \frac{(C-1)kL-4S}{8} + \alpha_y \frac{4(C-1)+kLS}{8} \end{pmatrix} \tag{7}$$

Assuming that a solenoid inclination is the only error affecting trajectory, we get the uncompensated angles in the solenoid-BPM drift as $\theta_x = x'_c + x'_\alpha$ and $\theta_y = y'_c + y'_\alpha$, where x'_c and y'_c are given by Eq. (5) (with $\mathcal{X} = -(x_\alpha + x'_\alpha Z)$ and $\mathcal{Y} = -(y_\alpha + y'_\alpha Z)$), and $x_\alpha, x'_\alpha, y_\alpha$ and y'_α are given by Eq. (7).

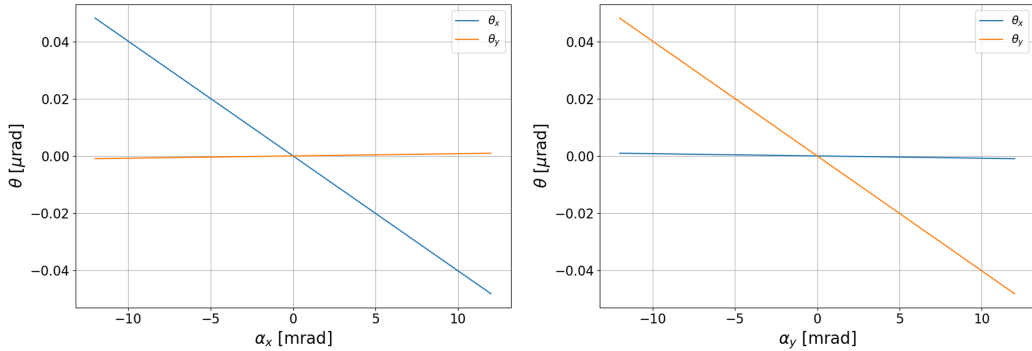


Figure 4: An uncompensated trajectory angle in a solenoid-BPM drift depending on an inclination of a solenoid.

Dependence of uncompensated angle on solenoid inclination is shown in Fig 4.

Notice, that according to the solenoids and correctors parameters given in Table 2, the maximum inclination that the correctors can compensate is $\alpha_{\max} = \frac{\chi c I_c(\max)}{B_s} \approx 12.5$ mrad. For inclinations $\alpha_{x,y} \leq \alpha_{\max}$ the error in an angle of compensated trajectory is minuscule. On the other hand, the experience with LEReC shows that the solenoids can be aligned with an accuracy better than 1 mrad. Therefore, it is reasonable to set the alignment requirement to that value.

2.3 Shifted solenoid

The effect of the shifted solenoid on electron beam trajectory is given by:

$$\vec{X}_d = M_s \begin{pmatrix} d_x \\ 0 \\ d_y \\ 0 \end{pmatrix} - \begin{pmatrix} d_x \\ 0 \\ d_y \\ 0 \end{pmatrix} = \begin{pmatrix} d_x \frac{C-1}{2} + d_y \frac{S}{2} \\ -d_x \frac{kS}{4} + d_y \frac{(C-1)k}{4} \\ -d_x \frac{S}{2} + d_y \frac{C-1}{2} \\ d_x \frac{(1-C)k}{4} - d_y \frac{kS}{4} \end{pmatrix} \quad (8)$$

where d_x, d_y are the transverse offsets with respect to the ideal e-beam trajectory.

Assuming that the solenoid shift is the only error, we can find the uncorrected angle of electron trajectory in the solenoid-BPM drift as $\theta_x = x'_c + x'_d$ and $\theta_y = y'_c + y'_d$, where x'_c and y'_c are given by Eq. (5) (with $\mathcal{X} = -(x_d + x'_d Z)$ and $\mathcal{Y} = -(y_d + y'_d Z)$), and x_d, x'_d, y_d and y'_d are given by Eq. (8).

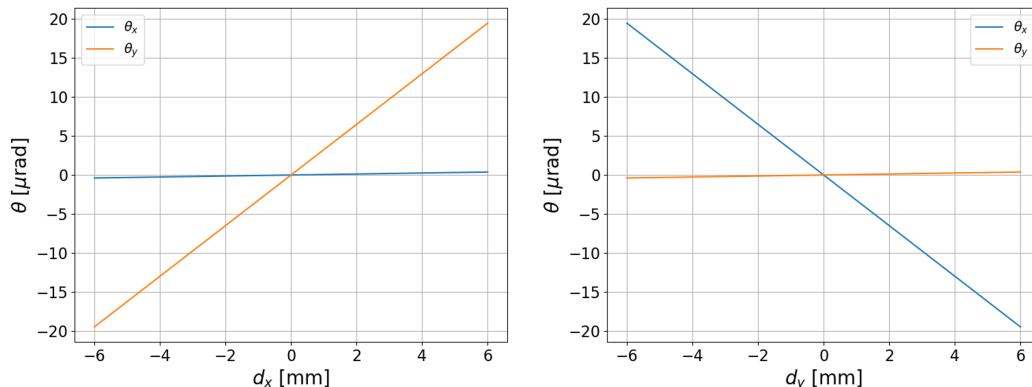


Figure 5: An uncompensated trajectory angle in a solenoid-BPM drift depending on the transverse shift of a solenoid.

Dependence of uncompensated trajectory angle on solenoid shift is shown in Fig 5. As one can see, if we align solenoids with transverse offsets not

exceeding $d_{x,y} = 1$ mm, then the total uncompensated trajectory angle will be $\sqrt{\theta_x^2 + \theta_y^2} \approx 4.5 \mu\text{rad}$.

2.4 Entering solenoid with misaligned trajectory

As we established above, a trajectory angle can not be compensated ideally. Additionally, one can have a shifted trajectory due to BPM errors. Therefore, even if the solenoid itself is ideally aligned, one might be entering it with a trajectory misalignment characterized by a vector $\vec{X}_{in} = (x_{in}, x'_{in}, y_{in}, y'_{in})^T$. The resulting trajectory at the exit of the solenoid is given by:

$$\vec{X}_{out} = M_s \vec{X}_{in} \quad (9)$$

The trajectory misalignment \vec{X}_{out} will not be ideally compensated, and thus, will cause misalignment in the following solenoid-BPM module.

Figure 6 demonstrates the effect of various trajectory misalignments at the entrance to a solenoid on an uncompensated trajectory angle in the following solenoid-BPM drift.

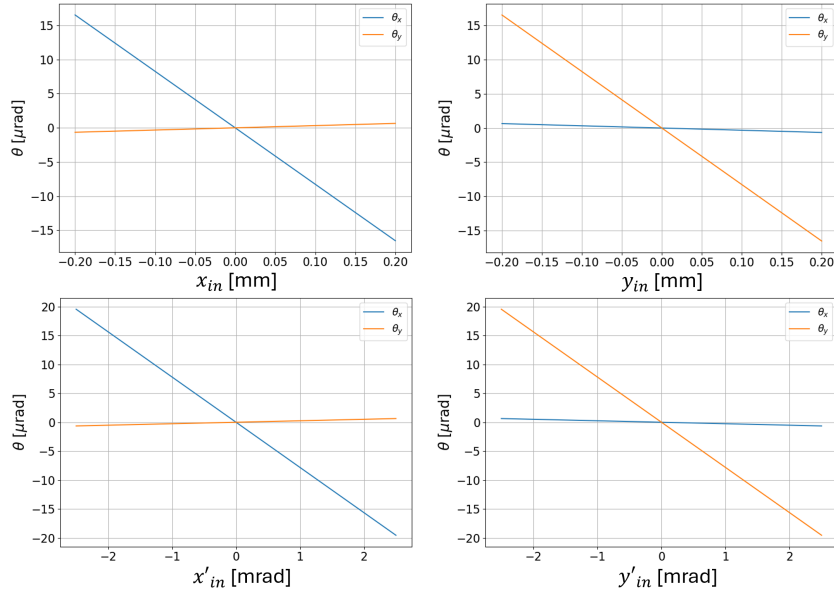


Figure 6: An uncompensated trajectory angle in the solenoid-BPM drift depending on various possible misalignments of the trajectory at the solenoid entrance.

The first observation one can make is that the uncompensated trajectory angle in the drift following the solenoid is two orders of magnitude smaller

than the trajectory angle at the entrance of this solenoid. This means that the suggested trajectory compensation scheme is quickly damping the trajectory angles as we move from one solenoid-BPM module to the next one.

The second observation is that the transverse offset of the trajectory at the solenoid entrance must not exceed a few tens of microns if one wants to keep an uncompensated trajectory angle in the following drift within a few microradians.

2.5 Misaligned BPMs

The errors in BPMs obviously result in uncompensated trajectory angles. Here, we will consider a simple model of both a BPM immediately upstream of a solenoid (BPM 1) and a BPM downstream of the solenoid (BPM 2 separated from the solenoid by a drift of length Z) having the position reading errors (x_{BPM}, y_{BPM}) of the same value but different sign. That is, we will assume that $x_{BPM1} = y_{BPM1} = -x_{BPM2} = -y_{BPM2}$.

With the outlined assumptions we get $\mathcal{X} = -(x_1 + x'_1 Z + x_{BPM})$, and $\mathcal{Y} = -(y_1 + y'_1 Z + y_{BPM})$, where $(x_1, x'_1, y_1, y'_1)^T = M_s \cdot (-x_{BPM}, 0, -y_{BPM}, 0)^T$. Substituting \mathcal{X} and \mathcal{Y} into Eq. (5) we get the trajectory angular errors in the solenoid-BPM drift as $\theta_x = x'_c + x'_1$ and $\theta_y = y'_c + y'_1$.

Figure 7 shows the dependence of trajectory angles on the value of BPMs' errors. One can see that, for example, for $x_{BPM} = y_{BPM} = 50 \mu\text{m}$, the total trajectory misalignment is $\theta = \sqrt{\theta_x^2 + \theta_y^2} \approx 12 \mu\text{rad}$.

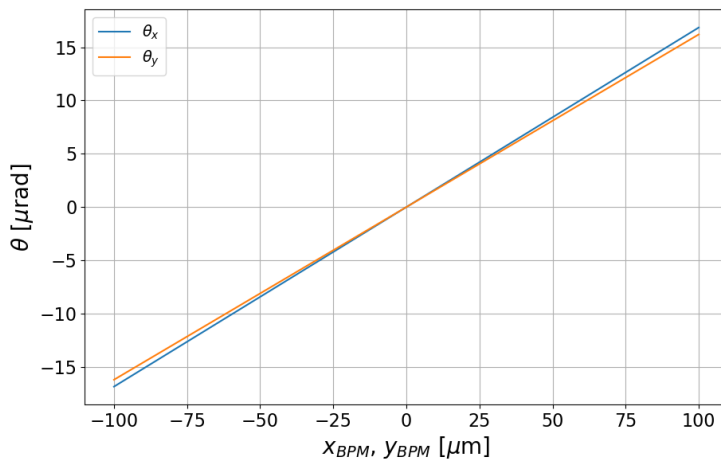


Figure 7: A dependence of trajectory angles on the BPMs' errors.

2.6 Fields in solenoid-BPM drift

We expect two types of fields in the cooling section drifts. One is the dipole-like ambient field (B_{ax}, B_{ay}) , which we expect to suppress to below 1 mG. The other is the focusing field of the proton bunch.

For small deflections of electron trajectory from a center of a proton bunch, the effect of protons' space charge on e-bunch trajectory in the drift is described by [9] $x'' = -Kx/(2\sigma_p^2)$, $y'' = -Ky/(2\sigma_p^2)$. Here $K = \frac{2I_p}{I_A(\gamma\beta)^3}$, I_p is the current of the slice of a p-bunch probed by an electron bunch, and $I_A \approx 17000$ A is Alfvén current.

The equation of motion of e-beam trajectory in the CS drifts is:

$$\begin{aligned} x'' &= b_x - \kappa x \\ y'' &= b_y - \kappa y \\ b_x &= \frac{B_{ax}}{B\rho}, \quad b_y = \frac{B_{ay}}{B\rho}, \quad \kappa = \frac{K}{2\sigma_p^2} \end{aligned} \quad (10)$$

Then, solving Eq. (10) with initial conditions (trajectory out of the solenoid) x_0, x'_0, y_0, y'_0 , we get:

$$\begin{aligned} x &= \frac{b_x}{\kappa} + \left(x_0 - \frac{b_x}{\kappa}\right) \cos(\sqrt{\kappa}s) + \frac{x'_0}{\sqrt{\kappa}} \sin(\sqrt{\kappa}s) \\ x' &= \left(\frac{b_x}{\sqrt{\kappa}} - \sqrt{\kappa}x_0\right) \sin(\sqrt{\kappa}s) + x'_0 \cos(\sqrt{\kappa}s) \\ y &= \frac{b_y}{\kappa} + \left(y_0 - \frac{b_y}{\kappa}\right) \cos(\sqrt{\kappa}s) + \frac{y'_0}{\sqrt{\kappa}} \sin(\sqrt{\kappa}s) \\ y' &= \left(\frac{b_y}{\sqrt{\kappa}} - \sqrt{\kappa}y_0\right) \sin(\sqrt{\kappa}s) + y'_0 \cos(\sqrt{\kappa}s) \end{aligned} \quad (11)$$

From Eq. (11), the trajectory angle averaged over the drift of the length Z is given by:

$$\begin{aligned} \theta_x &= \sqrt{\frac{1}{Z} \int_0^Z (x'(s))^2 ds} = \sqrt{x'_0 \cdot \frac{a_x(1-C_1)}{\kappa} + \frac{a_x^2(2Z-S_1)}{\kappa} + x'_0{}^2 \cdot \frac{2Z+S_1}{4}} \\ \theta_y &= \sqrt{\frac{1}{Z} \int_0^Z (y'(s))^2 ds} = \sqrt{y'_0 \cdot \frac{a_y(1-C_1)}{\kappa} + \frac{a_y^2(2Z-S_1)}{\kappa} + y'_0{}^2 \cdot \frac{2Z+S_1}{4}} \\ C_1 &\equiv \cos(2\sqrt{\kappa}Z), \quad S_1 \equiv \frac{\sin(2\sqrt{\kappa}Z)}{\sqrt{\kappa}}, \quad a_x \equiv \frac{b_x - \kappa x_0}{2}, \quad a_y \equiv \frac{b_y - \kappa y_0}{2} \end{aligned} \quad (12)$$

Let us assume that the fields in a drift are the only source of the trajectory misalignment. Then, initially, without trajectory correction, i.e. with correctors off we have from Eq. (11):

$$\begin{aligned} \mathcal{X} &= -\left(\frac{b_x}{\kappa} - \frac{b_x}{\kappa} \cos(\sqrt{\kappa}Z)\right) \\ \mathcal{Y} &= -\left(\frac{b_y}{\kappa} - \frac{b_y}{\kappa} \cos(\sqrt{\kappa}Z)\right) \end{aligned} \quad (13)$$

In our trajectory correction algorithm we assume that the distance from a solenoid to the following BPM is a true drift, that is we ignore fields in the drift. Hence, the correctors' settings are given by Eq. (5) with \mathcal{X} , \mathcal{Y} given by Eq. (13).

The true trajectory in the drift will be given by Eq. (11) with $(x_0, x'_0, y_0, y'_0) = (x_c, x'_c, y_c, y'_c)$ defined by Eq. (5), and with average angles in the drift given by Eq. (12).

Following the outlined analysis and assuming I_p for the central slice of the p-bunch (see Fig. 2) we can plot the dependence of $\langle\theta_{x,y}\rangle$ in the solenoid-BPM drift on $B_{a(x,y)}$. For the plot shown in Fig. 8 we assume that the uncompensated ambient field is directed along B_x and that it is constant over the length of the drift.

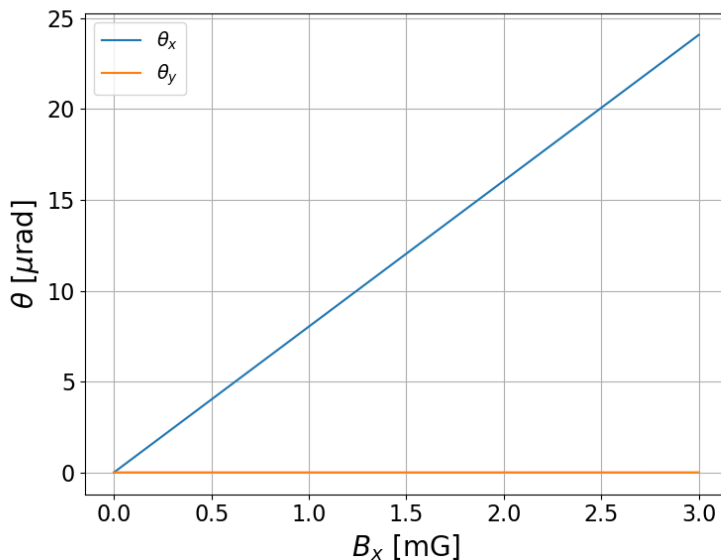


Figure 8: A dependence of average trajectory angle in the solenoid-BPM drift on the value of transverse uncompensated ambient field.

We must notice that for small trajectory displacements the effect of proton-electron space charge kick is very small and uncompensated trajectory angles are almost exclusively determined by transverse ambient field. Nonetheless, it is important to use the complete formulas (11) because in the presence of other errors over the length of the whole cooling section the effect of beam-beam kick can become noticeable. This point will be discussed more in the next chapter.

3 Expected angles in the cooling section

3.1 Model of cooling section

In the model of the cooling section we assume that the solenoids can be both shifted (with displacements d_x and d_y) and inclined (with angles α_x and α_y) with respect to the ideal trajectory set by the proton beam in the CS. We also assume that the e-beam position measured by a BPM have errors x_{BPM} , y_{BPM} . The proton beam with parameters listed in Table 1 is present and produces beam-beam kick. Finally, the transverse ambient field is given by its components B_{ax} and B_{ay} and is constant over the whole length of the cooling section.

We will assume that both solenoids and BPMs can be aligned with respect to the ideal e-beam trajectory with some accuracy. We further postulate that the accuracy of alignment A means that respective parameter has a random uniform distribution within $[-A, A]$. For example, if solenoid shift can be controlled with accuracy d_{\max} , then the probability that a solenoid n has shifts d_{nx} and d_{ny} is given by:

$$\mathcal{U}(-d_{\max}, d_{\max}) = \begin{cases} \frac{1}{2d_{\max}}, & d_{n(x,y)} \in [-d_{\max}, d_{\max}] \\ 0, & d_{n(x,y)} \in (-\infty, -d_{\max}) \vee (d_{\max}, \infty) \end{cases} \quad (14)$$

The correction algorithm assumes that the motion in the solenoids-BPMs drifts is unaffected by either ambient fields or BBK and sets correctors in module n according to Eq. (5) with \mathcal{X} , \mathcal{Y} defined by Eq. (11) (with all the errors taken into account):

$$\begin{aligned} \mathcal{X}_{n+1} &= - \left(\frac{b_x}{\kappa} + \left(x_n - \frac{b_x}{\kappa} \right) \cos(\sqrt{\kappa}Z) + \frac{x'_n}{\sqrt{\kappa}} \sin(\sqrt{\kappa}Z) + x_{(n+1)BPM} \right) \\ \mathcal{Y}_{n+1} &= - \left(\frac{b_y}{\kappa} + \left(y_n - \frac{b_y}{\kappa} \right) \cos(\sqrt{\kappa}Z) + \frac{y'_n}{\sqrt{\kappa}} \sin(\sqrt{\kappa}Z) + y_{(n+1)BPM} \right) \\ \vec{X}_n &= \vec{X}_{d(n)} + \vec{X}_{\alpha(n)} + \vec{X}_{out(n)} \end{aligned} \quad (15)$$

where $\vec{X}_{\alpha(n)}$, $\vec{X}_{d(n)}$ and $\vec{X}_{out(n)}$ are given by Eqs. (7), (8) and (9), and $\vec{X}_{out(n)}$ is a result of uncompensated trajectory errors $\vec{X}_{in(n)}$ at the entrance of the solenoid number n .

3.2 Sanity checks

We performed numerous tests to ensure the validity of the described CS model. Results of a few of these sanity checks are shown in this section.

Figure 9 shows an uncompensated e-beam trajectory entering the CS with horizontal angle $x'_0 = 50 \mu\text{rad}$ and affected only by the beam-beam

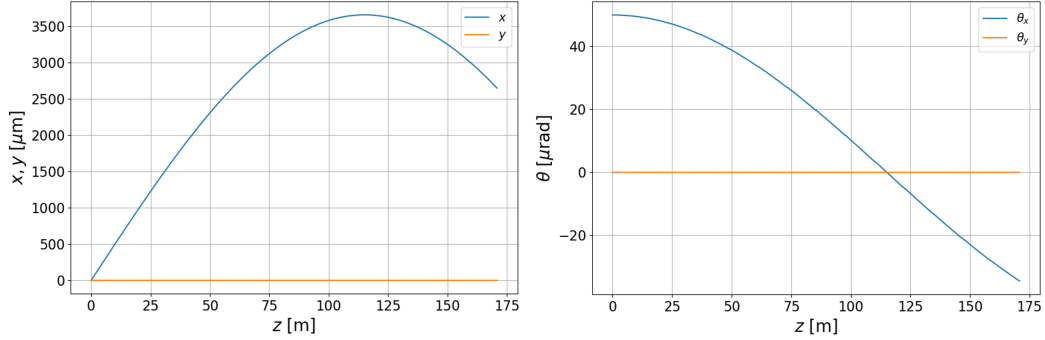


Figure 9: Uncompensated e-beam trajectory in presence of protons. Solenoids and correctors are off. No other errors are present.

kick. The solenoids, correctors and ambient fields are turned off and no other errors are present in these simulations. As one expects, according to Eq. (11) the trajectory through the CS is a simple oscillation described by:

$$x = \frac{x'_0}{\sqrt{\kappa}} \sin(\sqrt{\kappa}s), \quad x' = x'_0 \cos(\sqrt{\kappa}s) \quad (16)$$

Notice that the wavelength associated with BBK effect is rather long $\lambda_{BBK} = \frac{2\pi}{\sqrt{\kappa}} \approx 456$ m.

Electron beam trajectory under the conditions described above but now with solenoids set to their nominal strengths is shown in Fig. 10. As expected, the solenoids introduce $x - y$ coupling and reduce the oscillation's wavelength.

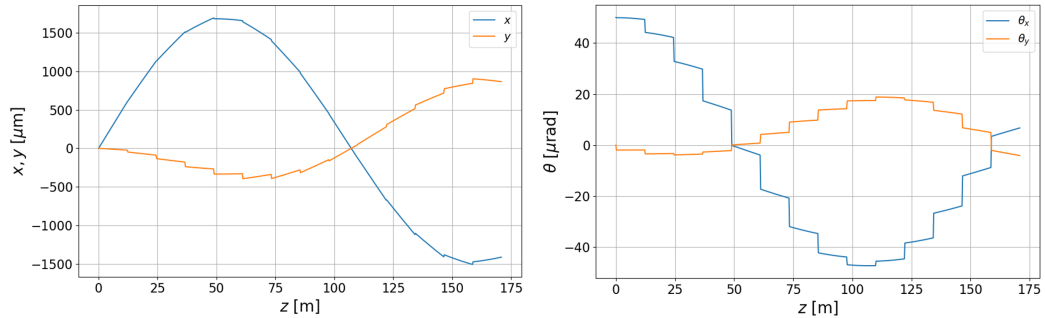


Figure 10: Uncompensated e-beam trajectory in presence of protons with solenoids at nominal currents. No other errors are present.

In next test we consider electron beam motion in an ambient field $B_{ax} = 1 \cdot 10^{-3}$ G, $B_{ay} = 0$ G. We assume that the protons are absent and that there are no misalignment errors in the CS. Figure 11 shows a well expected

parabolic trajectory in each drift, which is immediately obtained from Eq. (11) in the limit of $\kappa \rightarrow 0$:

$$\begin{aligned} x &= x_0 + x'_0 s + \frac{b_x}{2} s^2 \\ x' &= x'_0 + b_x s \end{aligned} \quad (17)$$

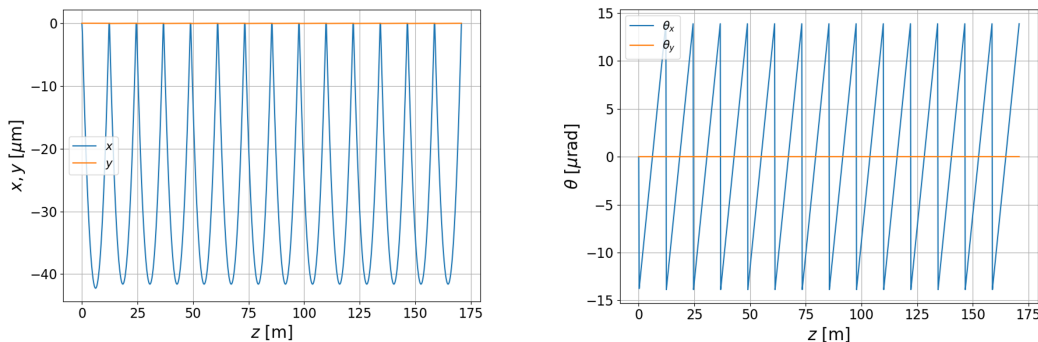


Figure 11: Compensated e-beam trajectory in presence of a uniform horizontal ambient field. No other errors are present.

Notice that the trajectory in the first drift in Fig. 11 differs from the other drifts trajectories because initial conditions for this drift are different. Electrons enter the first solenoid with zero angle, while other solenoids in the CS are entered at an angle of $\approx \frac{b_x Z}{2}$.

For another validity test we take the setup of the last example and add the errors in solenoidal shifts to our model. The shifts are randomly distributed according to Eq. (14) with $d_{\max} = 1$ mm in both the horizontal and vertical directions. Figure 12 shows the resulting corrected trajectory in the cooling section.

3.3 Average angles depending on combination of errors

Now we will assume that all the errors discussed in the previous chapter are present simultaneously.

Figure 13 shows corrected trajectory in the cooling section where the errors of solenoids and BPMs have random distributions of the kind discussed in Section 3.1. The accuracy of solenoids alignment is $d_{x_{\max}} = d_{y_{\max}} = 1$ mm and $\alpha_{x_{\max}} = \alpha_{y_{\max}} = 1$ mrad. This level of alignment is very well achievable with a mechanical survey, as confirmed by LEReC experience. The BPMs readings have accuracy $x_{BPM_{\max}} = y_{BPM_{\max}} = 50$ μm . The uncompensated ambient field is uniform throughout the CS and has value $B_{ax} = 1$ mG,

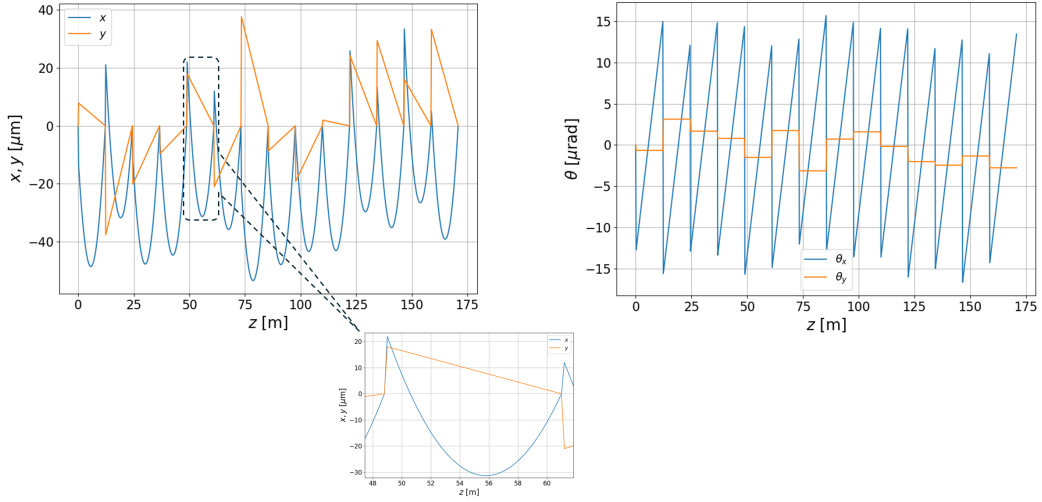


Figure 12: Compensated e-beam trajectory in presence of a uniform horizontal ambient field and random shifts of the CS solenoids. No other errors are present. The bottom plot shows a zoomed view of a trajectory in a single solenoid-BPM module.

$B_{ay} = 1$ mG. The proton beam with the parameters listed in Table 1 is present in the CS.

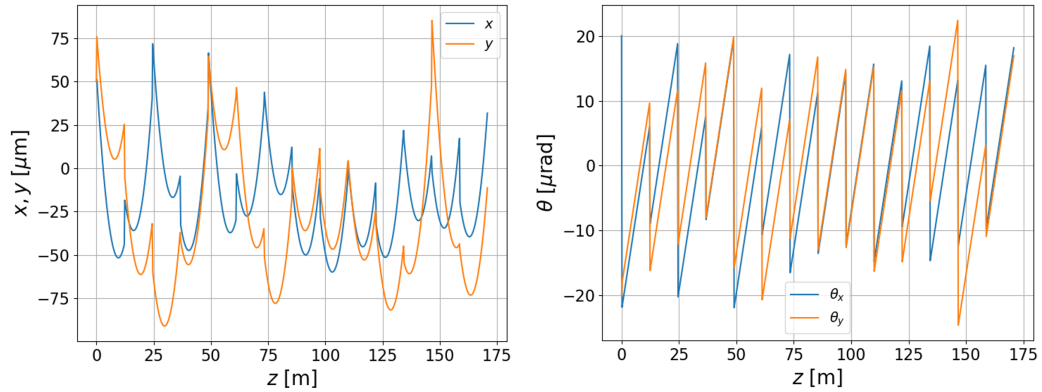


Figure 13: Compensated e-beam trajectory in presence of randomly distributed alignment errors, ambient fields, and proton-electron kick. The beam enters the CS with $x_0 = y_0 = 50 \mu\text{m}$ and $x'_0 = -y'_0 = 20 \mu\text{rad}$.

Based on the simulations described above we can calculate the average angles in each of the drifts (in a drift number n we denote the average x, y angles as $\theta_{x_n}, \theta_{y_n}$) according to Eq. (12). Then the average total angle in the cooling section is given by:

$$\langle \theta \rangle = \sqrt{\frac{1}{N_{drift}} \sum_{n=1}^{N_{drift}} \theta_n^2} \quad (18)$$

$$\theta_n^2 = \theta_{x_n}^2 + \theta_{y_n}^2$$

where number of solenoid-BPM drifts in the CS $N_{drift} = 14$.

Figure 14 gives average angles in the CS corresponding to simulations results shown in Fig. 13.

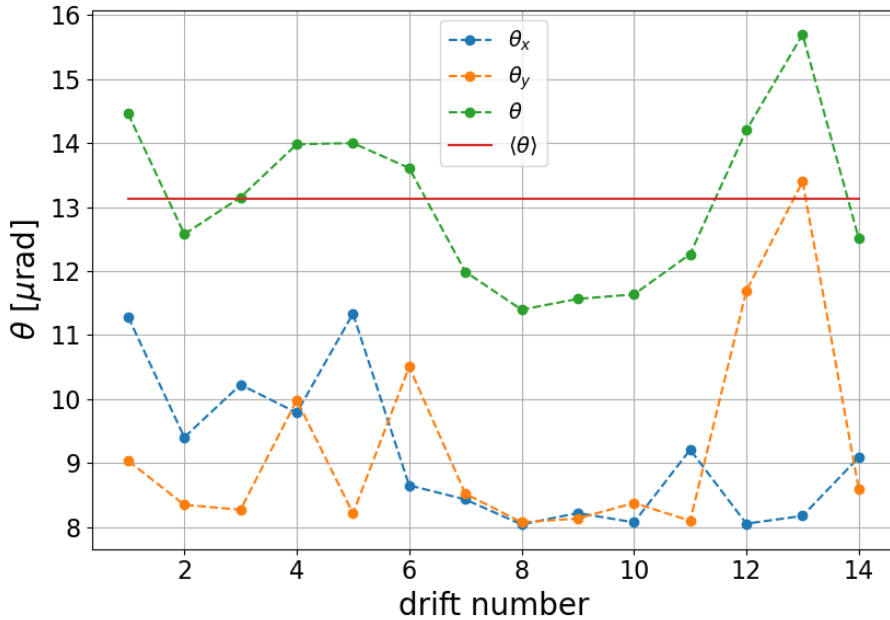


Figure 14: Average angles in the cooling section corresponding to e-beam trajectory shown in Fig. 13.

Finally, we repeat the described simulations hundred thousand times (i.e. we “generate” $N = 10^5$ cooling sections with random errors) and plot the probability distribution function $p(\langle \theta \rangle)$ of average total trajectory angle in the CS. We define the probability of getting an average trajectory angle within limits $\langle \theta \rangle \in [\theta_{smaller}, \theta_{larger}]$ as:

$$P = \frac{1}{N} \int_{\theta_{smaller}}^{\theta_{larger}} p(\langle \theta \rangle) d\langle \theta \rangle \quad (19)$$

The results of such studies performed for alignment accuracies outlined at the beginning of this section are shown in Fig. 15.

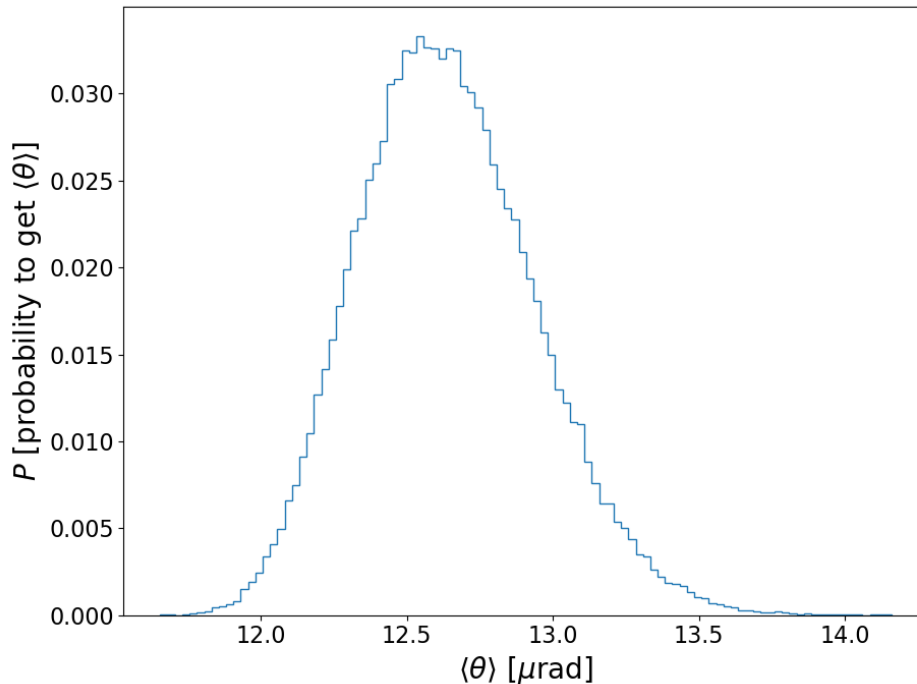


Figure 15: Probability of getting a particular trajectory misalignment angle in the CS.

As one can see, for the given accuracy of solenoids and BPM alignments in the presence of uncompensated ambient fields and proton-electron kick, the most probable trajectory misalignment angle is $\langle\theta\rangle \approx 12.6 \mu\text{rad}$. At the same time the “large misalignment tale” of the distribution reaches $\max(\langle\theta\rangle) \approx 14.2 \mu\text{rad}$, which is still less than the maximum tolerable misalignment $\theta_{\text{max}} = 20 \mu\text{rad}$.

We repeat these studies for various combinations of ambient fields and BPM reading accuracies. The results are summarized in Table 3.

4 Conclusion and discussion

We developed a model for the electron beam trajectory alignment in the cooling section of the EIC Low Energy Cooler.

Table 3: Trajectory misalignment depending on CS parameters (proton-electron kick is taken into account)

| | | | | | | | | |
|--|------|------|------|------|------|------|------|------|
| $d_{x_{\max}} = d_{y_{\max}}$ [mm] | 1 | | | | | | | |
| $\alpha_{x_{\max}} = \alpha_{y_{\max}}$ [mrad] | 1 | | | | | | | |
| $B_{ax} = B_{ay}$ [mG] | 0.5 | 1 | 1 | 1 | 1.5 | 1.5 | 1.5 | 2 |
| $x_{BPM_{\max}} = y_{BPM_{\max}}$ [μm] | 100 | 50 | 75 | 100 | 50 | 75 | 100 | 0 |
| most probable $\langle\theta\rangle$ [μrad] | 11.3 | 12.6 | 13.7 | 14.9 | 17.9 | 18.6 | 19.5 | 22.9 |
| $\max(\langle\theta\rangle)$ [μrad] | 16.3 | 14.2 | 16.4 | 18.7 | 19.1 | 20.6 | 23.0 | 23.1 |

The model includes randomly distributed misalignments of the CS solenoids (shifts and inclinations) and errors in BPMs readings. It also takes into account both the remnant ambient field and the proton-electron trajectory kick induced by protons space charge.

This model allowed us to explore dependence of expected e-beam trajectory misalignment on various factors. The results of the studies are summarized in Table 3.

The immediate conclusion that one can make from obtained results is that it is important to suppress the ambient transverse fields in the CS drifts to:

$$B_{\perp} = \frac{1}{Z} \int_0^Z \sqrt{B_{ax}^2(z) + B_{ay}^2(z)} dz \approx 1.4 \text{ mG} \quad (20)$$

Then the requirements to the accuracy of BPM readings become rather forgiving, one can allow $x_{BPM_{\max}}$ and $y_{BPM_{\max}}$ of up to 100 μm . Yet, the case of $B_{\perp} \leq 1.4 \text{ mG}$ and $x_{BPM_{\max}} = y_{BPM_{\max}} = 50 \mu\text{m}$ seems to be the most attractive trade-off between overall requirements to field shielding and BPMs accuracy.

The model presented in this paper can be further applied to studies of optimal CS configurations (such as shielding requirements vs. length of the drifts), and derivation of requirements to the LEC feedback system.

References

- [1] G. I. Budker, An effective method of damping particle oscillations in proton and antiproton storage rings, *At. Energ.* 22, 346 (1967) [*Sov. At. Energy* 22, 438 (1967)].

- [2] S. Seletskiy et al., Accurate setting of electron energy for demonstration of first hadron beam cooling with RF accelerated electron bunches, *Phys. Rev. Accel. Beams* 21, 111004 (2019).
- [3] A. Fedotov et al., Experimental demonstration of hadron beam cooling using radio frequency accelerated electron bunches , *Phys. Rev. Lett.* 124, 084801 (2020).
- [4] D. Kayran et al., High brightness electron beams for linac based bunched beam electron cooling, *Phys. Rev. Accel. Beams* 23, 021003 (2020).
- [5] X. Gu et al., Stable operation of a high voltage high current dc photoemission gun for the bunched beam electron cooler in RHIC, *Phys. Rev. Accel. Beams* 23, 013401 (2020).
- [6] S. Seletskiy et al., Obtaining transverse cooling with non magnetized electron beam, *Phys. Rev. Accel. Beams* 23, 110101 (2020).
- [7] A. Jain, Results of Magnetic Measurements in LEReC Solenoids (2015). [https://www.c-ad.bnl.gov/esfd/LE_RHICeCooling_Project/2015Meetings/11_24_15_\(Jain\)LEREC-SolenoidMeasurements_Rev.pdf](https://www.c-ad.bnl.gov/esfd/LE_RHICeCooling_Project/2015Meetings/11_24_15_(Jain)LEREC-SolenoidMeasurements_Rev.pdf)
- [8] S. Seletskiy et al., Finalized configuration of magnetic shielding for LEReC Cooling Section, BNL-114736-2017-IR, (2017).
- [9] S. Seletskiy et al., Effect of beam-beam kick on electron beam quality in first bunched electron cooler, *J. Phys.: Conf. Ser.* 1350 012134 (2019).
- [10] S. Seletskiy et al., Strategy for alignment of electron beam trajectory in LEReC cooling section, BNL-112720-2016-IR, (2016).
- [11] S. Seletskiy et al., Alignment of electron and ion beam trajectories in nonmagnetized electron cooler, TUPAB145, roceedings of IPAC2017, Copenhagen, Denmark (2017)
- [12] S. Seletskiy, Attainment of Electron Beam Suitable for Medium Energy Electron Cooling, PhD. Thesis, (2005). <https://doi.org/10.2172/878935>